Decomposition of powerful axisymmetrically polarized laser pulses in underdense plasma

Nobuhiko Nakanii,[1,2,3,*] Tomonao Hosokai,[1,2,4] Naveen C. Pathak,[1] Shinichi Masuda,[1,2] Alexei G. Zhidkov,[1,2] Hiroki Nakahara,[4] Kenta Iwasa,[4] Yoshio Mizuta,[4] Naoki Takeguchi,[4] Takamitsu P. Otsuka,[1] Keiichi Sueda,[1] Jumpei Ogino,[1] Hirotaka Nakamura,[4] Michiaki Mori,[3] Masaki Kando,[3] and Ryosuke Kodama[1,4,5]

[1]*Photon Pioneers Center, Osaka University*

[2]*Core Research of Evolutional Science and Technology (CREST), Japan Science and Technology Agency*

[3]*Kansai Photon Science Institute, National Institutes for Quantum and Radiological Science and Technology*

[4]*Graduate School of Engineering, Osaka University*

[5]*Institute of Laser Engineering, Osaka University*

(Received 2 November 2015; revised manuscript received 9 August 2016; published 19 December 2016)

Interaction of relativistically intense axisymmetrically polarized (radially or azimuthally polarized) laser pulses (RIAPLP) with underdense plasma is shown experimentally and theoretically to be essentially different from the interaction of conventional Gaussian pulses. The difference is clearly observed in distinct spectra of the side-scattered laser light for the RIAPLP and Gaussian pulses, as well as in the appearance of a spatially localized strong side emission of second harmonic of the laser pulse in the case of RIAPLP. According to our analysis based on three-dimensional particle-in-cell simulations, this is a result of instability in the propagation of RIAPLP in uniform underdense plasma.

DOI: 10.1103/PhysRevE.94.063205

The quality of laser field distribution is a key part of any laser technique. For example, Gaussian-shape laser pulses are widely used for laser wake-field acceleration (LWFA) [1–9] because of their high quality. Propagation of Gaussian laser pulses in underdense plasma was a matter of study for decades. Self-focusing, filamentation, and hosing are well investigated for high-power short laser pulses with the Gaussian profile [10–12]. However, some laser modes may be useful for controllable electron self-injection, further electron acceleration, and/or probing of quality of plasma optics [13–16]. Here, axisymmetrically polarized, radially (E_r, B_ϕ) or azimuthally polarized (E_ϕ, B_r), laser pulses are of particular interest being two TEM01 or TEM10 modes, the nearest to Gaussian (TEM00) mode. Such modes when tightly focused have been proposed theoretically for the electron vacuum acceleration [17–19] and for efficient electron and positron wake-field acceleration [20]. However, the propagation of relativistically intense axisymmetrically polarized laser pulses (RIAPLP) in underdense plasma has particularly interest in view of existence of different laser mode in plasma. To our knowledge, the effects of propagation such pulses in underdense plasma have yet to be examined both theoretically and experimentally.

The intensity of axisymmetrically polarized laser pulses has a donut shape in a pulse focal spot. The transverse ponderomotive force of the RIAPL, acting towards the laser axis, can collect large number of electrons into the central limited area of the spot [20,21]. The increase of charge density of electron beam can be expected due to injecting these massive electrons to wake field excited by another laser pulse in staging acceleration [22–24]; on the other hand, the electron compression at the laser axis can cause instability, the decomposition of the RIAPL, as predicted in Ref. [21].

In this paper, we demonstrate experimental proof of the RIAPLP decomposition, which is manifested in strong side emission of second harmonics generation from the compressed high-density electrons. This is also shown via spectral analysis of laser electric field using three-dimensional (3D) relativistic particle-in-cell simulation.

The experimental setup is shown in Fig. 1(a). This experiment has been performed with a 40-TW Ti:Sapphire laser system (Amplitude Technologies) at Photon Pioneers Center, Osaka University based on a chirped pulse amplification (CPA) technique. The pulse energy on target was 660 mJ and the pulse duration was 50 fs. The central wavelength of the laser pulse is 800 nm. The contrast ratio between the main pulse and the nanosecond prepulse caused by the amplified spontaneous emission (ASE) is $\sim 10^{10}$. The contrast at 1 ps and 10 ps before the peak of main pulse is $\sim 10^5$ and 10^9, respectively. Those are measured by a third-order cross correlator (SEQOIA, Amplitude Technology). The maximum laser intensity of the RIAPLP on the target is estimated to be 3×10^{19} W/cm^2. A linearly polarized (horizontally polarized) laser pulse with diameter of $\sim$ 50 mm is converted to an axisymmetrically polarized laser pulse by passing through an eight-divided wave plate [25,26]. As shown in Fig. 1(b), the eight-divided wave plate consists of eight pieces of $1/2\ \lambda$ wave plate with different optical axis. Rotating the wave plate enables to switch the pulse polarization between radial, azimuth, and the spiral polarizations. The RIAPLP is focused at a distance of 100 μm inside from the front edge of the slit nozzle by a gold-coated off-axis parabolic mirror (OAP) with $f/3.6$ ($f = 177.8$ mm). The focal spot patterns in vacuum with and without using the eight-divided wave plate on target measured by the focal spot monitor are shown in Figs. 1(c) and 1(d), respectively. The focal spot of the RIAPLP has a clear donut shape, otherwise that of the relativistically intense linearly polarized laser pulse (RILPLP) has Gaussian shape.

The pulsed gas jet of helium is produced by a shock-wave-free slit nozzle and solenoid valve (Smartshell Co.). The shape of the nozzle exit is rectangular of 1.2 mm length and

*Present affiliation: Kansai Photon Science Institute, National Institutes for Quantum and Radiological Science and Technology; nakanii.nobuhiko@qst.go.jp

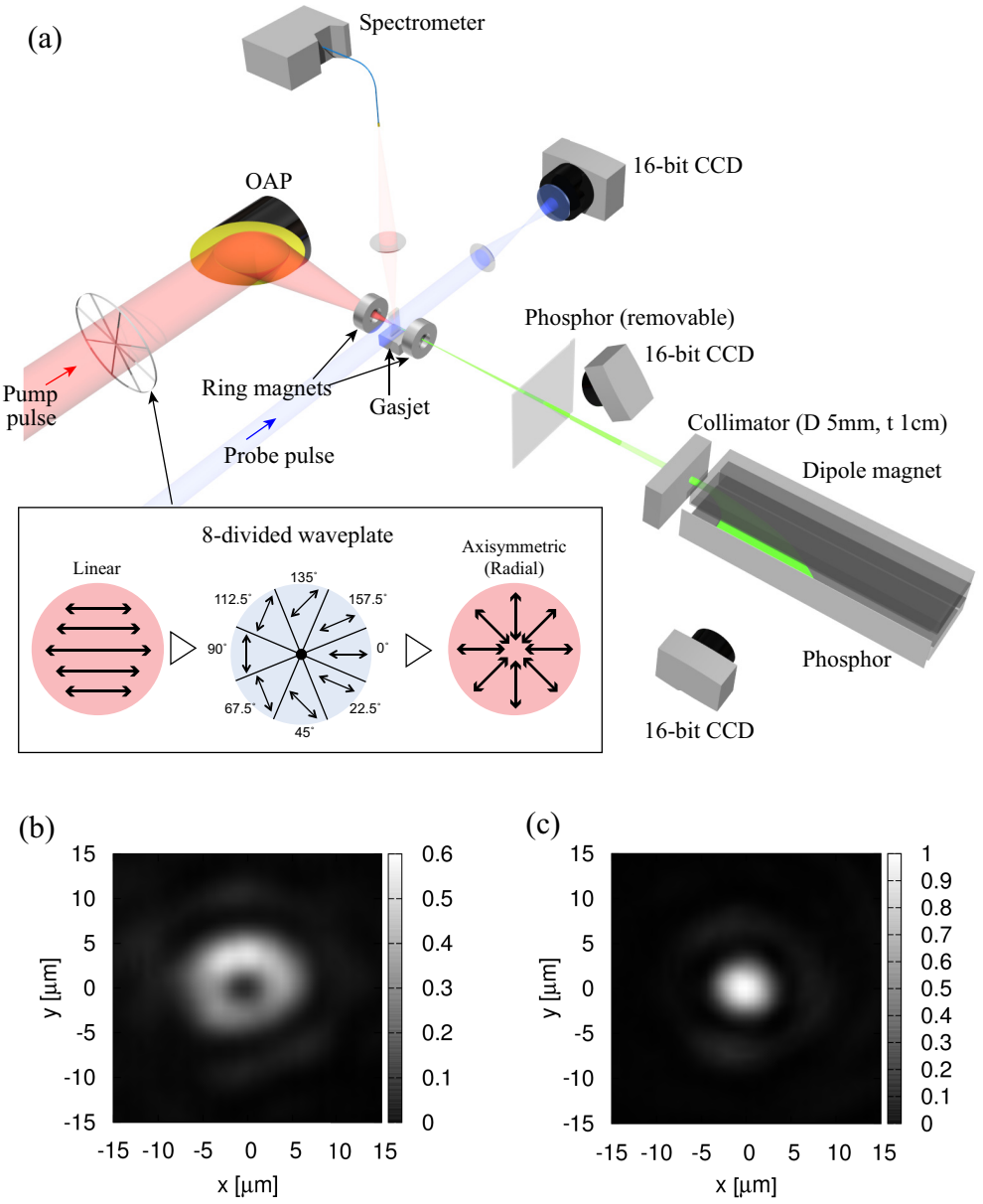

FIG. 1. (a) Experimental schematic. (b) Focus spot profile of RIAPLP with the eight-divided wave plate and (c) RILPLP without the wave plate.

4.0 mm width. The atomic density of the gas is estimated to be about 3.4×10^{19} cm^{-3}. The gas could be fully ionized by the laser pulse. A magnetic device that consists of two ring-shaped neodymium magnets applies external magnetic field ($B \sim 0.25$ T) in laser propagation direction [13–15]. The spatial distribution of ejected electron beams as an important characteristic of laser-plasma interaction was measured by a phosphor screen (Mitsubishi Chemical Co. LTD, DRZ-High) with diameter of 9 cm. The screen is located at 43 cm away from the gas jet target. The DRZ-High screen is sensitive to high-energy particles and radiations, so that the front side of the screen is laminated with a 12-μm-thick aluminum foil to avoid exposure to the laser pulses, scattering lights, and low-energy electrons. An electron spectrometer using a dipole magnet measures the energy spectrum of the beams. The energy-resolved electrons turned by the dipole magnet ($B \sim 0.25$ T) irradiates to another phosphor screen. A 1-cm-thick aluminum collimator with 5-mm-diameter hole is placed in front of the electron spectrometer. The scintillating images on these phosphor screens made by the deposited electrons are recorded by charged coupled device (CCD) cameras (Bitran Co., BU-51LN) with a commercial photographic lens from the backside of the screen. To reduce the background noise due to scattering light of laser pulses, band-pass filters (BG-39, $\lambda = 360$–580 nm) are set at the front of the cameras.

The pulse with a few percent of the laser energy was split by a pellicle and is converted to second harmonic ($\lambda \sim 400$ nm, $\tau \sim 50$ fs) by beta-barium borate (β-BaB_2O_4, BBO) crystal. This second harmonic is used as probe pulse to observe the condition of plasma by shadowgraph imaging from the side. At the upper side of the gas jet, an optical spectrometer is placed to observe spectrum of the side scattering from the

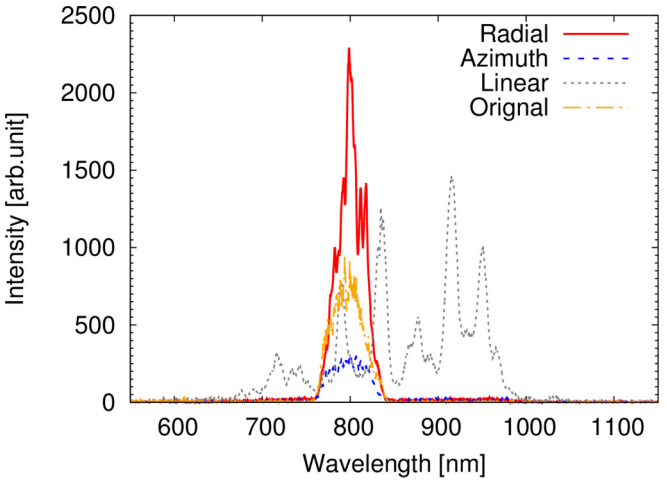

FIG. 2. Spectra of side scattering by using the radially, azimuthally, and linearly polarized pulses and the original spectrum of the laser pulse with pulse energy of 660 mJ.

laser plasma interactions. The spectral range of the optical spectrometer is from 520–1180 nm.

Figure 2 shows spatially and temporally integrated spectra of side scattering to the normal direction of the laser axis caused by interaction of RIAPLP or RILPLP with gas jets. One can see significant difference between spectra from RIAPLP and RILPLP, which is a result of inequality in RIAPLP and RILPLP propagation in underdense plasma. While the spectrum generated by an RILPLP is a typical for LWFA reflecting the strong red shift owing to formation of a plasma wave in the laser wake [27] and the self-phase modulation by the plasma wave because the pulse width is much longer than the wavelength of plasma wave [28], the spectrum of the RIAPLP is slightly broadened around the fundamental wavelength. The bandwidth of the scattering light caused by the RIAPLP is almost same as that of the original laser pulse. No signature of wake formation is seen for RIAPLP. However, it may be the effect of pulse decomposition: if the RIAPLP decomposes during its propagation the scattering light with the red shift may be too weak for detection.

Another sign of RIAPLP decomposition during its propagation is exhibited by Fig. 3 where Figs. 3(a)–3(c) are shadowgraph images of the plasmas created by RIAPLP and RILPLP with a probe pulse (∼ 400 nm) and Figs. 3(d)–3(e) show their profiles after transmission through horizontal polarizer. The probe pulse has the transverse polarization. Figures 3(a), 3(d); 3(b), 3(e); and 3(c), 3(f) show those in the cases of radial polarization, azimuth polarization, and linear polarization, respectively. In the shadowgraph images, one can see a strong second harmonic (SH) localized near the focus point of RIAPLP. This SH has been observed in either case of radial and azimuthal polarizations as shown in Figs. 3(d) and 3(e).

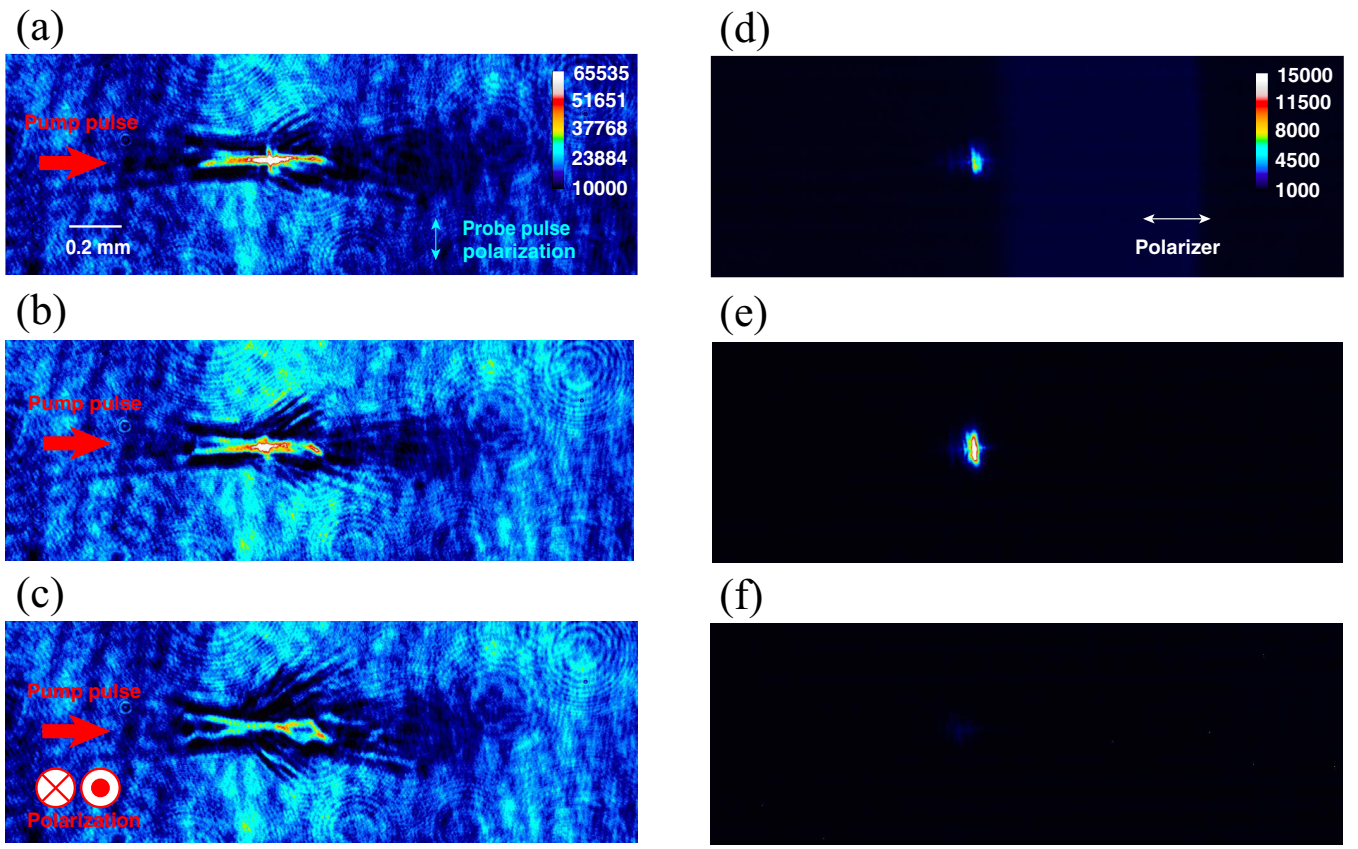

FIG. 3. (a)–(c) Shadowgraph images of the plasmas and (d)–(f) images of the second harmonic source obtained by filtering with polarizer. The probe pulse has the transverse polarization. (a), (d); (b), (e); and (c), (f) show the cases of radial polarization, azimuth polarization, and linear polarization, respectively.

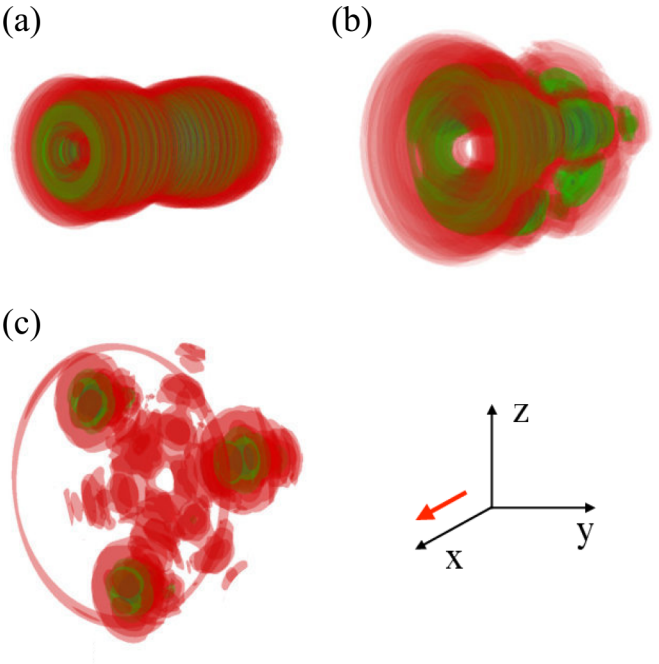

FIG. 4. 3D contour plots of intensity evolution of a radially polarized pulse propagating in uniform underdense plasma. The snapshots show intensity distribution at (a) 458 fs and (b) 817 fs, and (c) 1.86 ps. The x-y-z triad corresponds to the Cartesian coordinates of the simulation geometry and the arrow indicates the direction of propagation of the pulse.

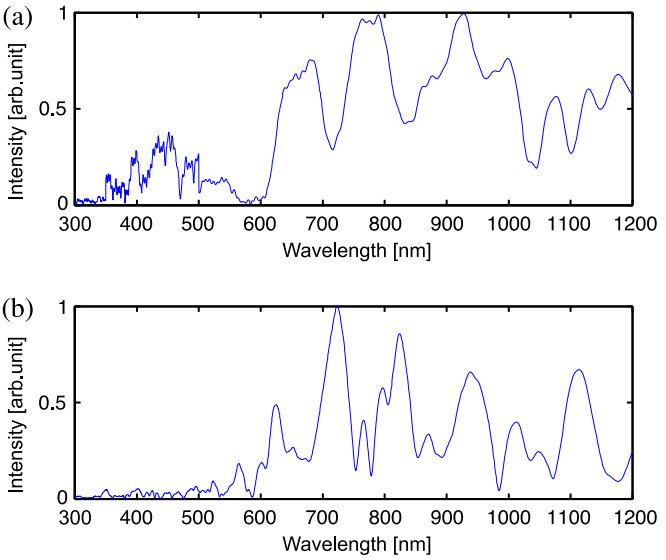

FIG. 5. (a) Spectrum of E_y component of the radially polarized laser pulse at 1.86 ps, and (b) spectrum of E_y component of the Gaussian laser pulse at 1.86 ps.

In contrast to SH emission reported in Ref. [29], in our experiments SH is observed in a quite short distance of about a few tens μm FWHM. In the case of RILPLP we did not observe such strong SH emission in all experiments. Since the probe pulse has the vertical linear polarization it cannot be transmitted through the horizontal linear polarizer as in Figs. 3(d)–3(f). Therefore, one can see the strong SH emission with different polarization with probe pulse in the cases of the RIAPLP.

To analyze the underlying mechanism of the RIAPLP propagation and its spectral modification, PIC simulation with FPLASER3D code [30] was performed. The laser pulse and plasma parameters were chosen close to those in the experiments. The axial resolution in the simulation is $\lambda/28$ and the transverse resolution is $\lambda/10$, and eight particles per cell, where λ is the wavelength of the laser pulse. The plasma length is set to 1 mm, with density gradient of length 120 μm on either edge. The focus position of the pulse is 100 μm inside the simulation box. Figure 4 shows snapshots of the intensity evolution of a radially polarized laser pulse propagating in uniform underdense plasma. Figure 4(a) correspond to 458 fs or 137.4 μm, Fig. 4(b) correspond to 817 fs or 245.1 μm, and Fig. 4(c) corresponds to 1.86 ps or 558 μm. Simulations reveal that owing to the donut shape of the electric field of the RIAPLP, the electron density is compressed along the axial direction. The compressed electron density interacts with the laser pulse and provokes instability. As a result of the instability the laser pulse breaks down into filaments. The nature and detailed analysis of this instability can be found in Ref. [21]. Due to compression, the on-axis electron density approaches near critical density. Interaction of the laser pulse with such a high-density plasma ramp results in harmonic generation [31]. Emission of second harmonic light indirectly implies to the occurrence of the instability. The SH is generated along the density gradient, since the density gradient is perpendicular to the laser pulse direction, the SH emission is observed perpendicular to the pulse propagation direction.

We performed spectral analysis of the laser radiation as a key part of this research using fast Fourier transform (FFT). The y component of the laser electric field transformed from space domain to k domain, where k is the wave vector of the laser pulse. Mathematically, this can be written as $f(k) = \sum E_y(x)e^{i2\pi kx}dx$, i.e., the y component of the laser field is summed up along the y and z directions and reduced from three dimensions to one dimension. This total field is than transformed to spectrum using FFT. Figure 5(a) shows the simulated on-axis spectrum of the radially polarized pulse. The spectrum corresponds to Fig. 4(c). As expected, there is a clear signal of the second harmonic generation. One can notice that on the one side there is a modulation and progressive red shift of the laser pulse, which is a sign of wake-field generation, and on the other side, there is a quasiselective blue shift of the laser pulse, which is around second harmonic.

To confirm that the generation of the second harmonic radiation is typical for RIAPLP, we also performed simulation with Gaussian laser pulse. Figure 5(b) shows the on-axis spectrum for the Gaussian pulse at the same time as for the radially polarized laser pulse in Fig. 5(a). It displays that there is only red shift in the simulated spectrum, and no sign of strong second harmonic component. Thus, simulation supports the observation of second harmonic generation from RIAPLP in our experimental conditions.

Figure 6 shows spatial profiles of electron beams generated by the RIAPLP (radial and azimuth polarizations) and the RILPLP with pulse energies 660 mJ on target. As shown in Figs. 6(a) and 6(b), the divergence of the electron beam in the case of the RIAPLP is smaller than the RILPLP in

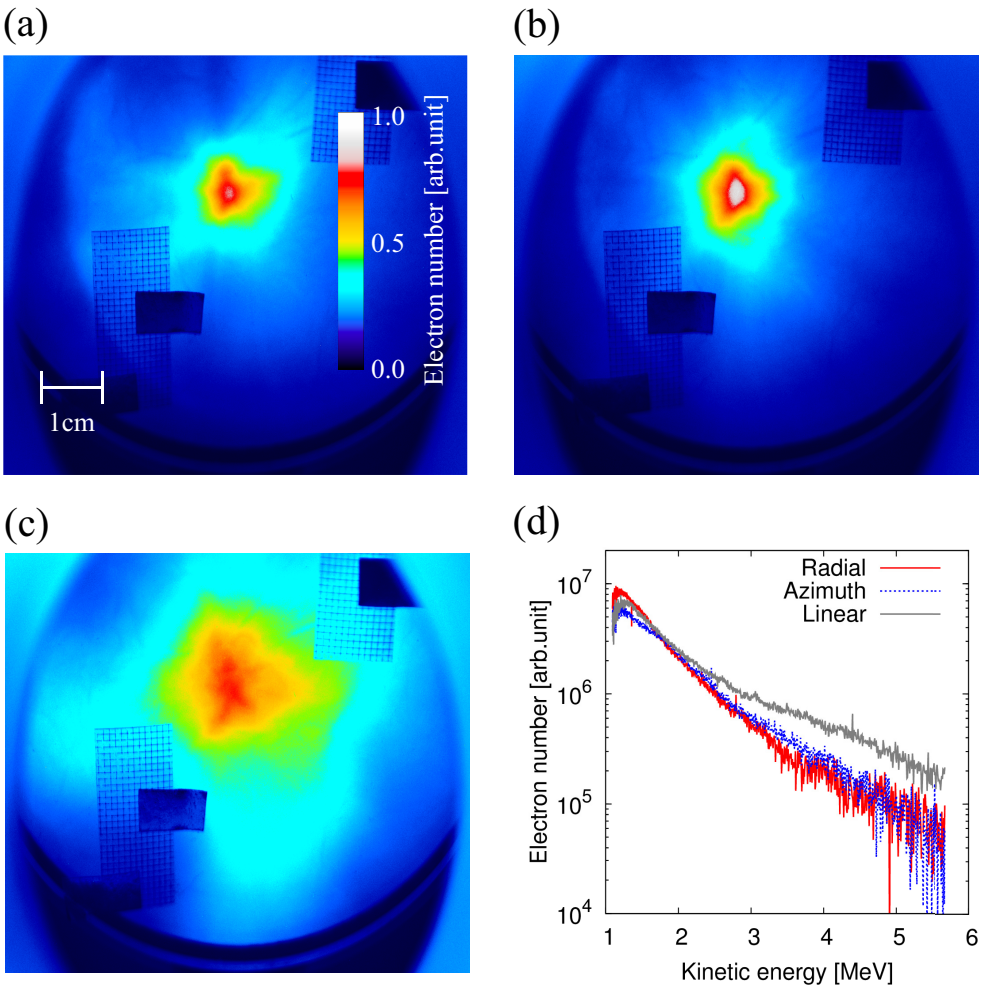

FIG. 6. Spatial profiles of electron beams in the case of (a) radial, (b) azimuthal, and (c) linear polarization with pulse energy of 660 mJ, and (d) energy spectra of electron beams for each polarization.

Fig. 6(c). The electron number on the center of beam produced by the RIAPLP is more than the RILPLP. Energy spectra of the electron beams with each polarization are also shown in Fig. 6(d). The temperature of the electron beam produced by the RIAPLP is lower than the RILPLP. This could be caused by slightly lower intensity of the RIAPLP than the RILPLP. In the acceleration by RIAPL, prepulse effect may drastically change the acceleration process: according to Ref. [21] there is no RIAPLP decomposition in plasma channels. In the present experiments we worked with a short-focus laser pulse and a short gas jet whose length is $\sim$ 1 mm. Therefore, in electron spectra we see distributions of self-injected electrons without further acceleration in the case of RIAPL. Since the electron self-injection occurs mostly in the vicinity of focus spot we observe no significant difference in LWFA with RILPLP and RIAPLP. An increase of gas jet length and the prepulse energy may drastically change this result.

In conclusion, we have found experimental proof of strong decomposition of axisymmetrically polarized laser pulses in underdense plasma. During the decomposition the strong SH is emitted in quite short distance. In the case of linearly polarized laser pulses SH emission does not occur. The SH emission confirms the electron compression near the laser axis that results in the pulse instability. Due to pulse decomposition no notable red shift was observed in time- and space-integrated spectra of scattering light. Therefore, no essential laser wake-field acceleration of plasma electrons has been observed. Detected MeV energy electrons are the results of wake wave decomposition only. However, RIAPLP can propagate in deep plasma channels without the decomposition [21]. This means that the RIAPLP can be used for probing the plasma optical elements [13–16]. For example, exit of RIAPLP from a plasma channel will be accompanied by a strong emission of SH, which is easy to detect.

The authors thank the reviewers for their fruitful and helpful comments and suggestions to improve this article. This work was supported by Core Research of Evolutional Science and Technology, Japan Science and Technology Agency (CREST, JST). It was also supported by Genesis Research Institute, Inc. This work was also funded by ImPACT Program of Council for Science, Technology and Innovation (Cabinet Office, Government of Japan). This work was partially supported by JSPS Core-to-Core Program on International Alliance for

Material Science in Extreme States with High Power Laser and XFEL from Ministry of Education, Culture, Sports Science and Technology (MEXT) of Japan. This work was also supported by the Large Scale Simulation Program No. 14/15-26 (FY2015) of High Energy Accelerator Research Organization (KEK).

[1] S. P. D. Mangles, C. D. Murphy, Z. Najmudin, A. G. R Thomas, J. L. Collier, A. E. Dangor, P. S. Foster, J. L. Collier, E. J. Divall, J. G. Gallacher, C. J. Hooker, D. A. Jaroszynski, A. J. Langley, W. B. Mori, P. A. Norreys, F. S. Tsung, R. Viskup, B. R. Walton, and K. Krushelnick, Nature (London) **431**, 535 (2004).

[2] C. G. R. Geddes, Cs. Toth, J. van Tilborg, E. Esarey, C. B. Schroeder, D. Bruhwiler, C. Nieter, J. Cary, and W. P. Leemans, Nature (London) **431**, 538 (2004).

[3] J. Faure, Y. Glinec, A. Pukhov, S. Kiselev, S. Gordienko, E. Lefebvre, J.-P. Rousseau, F. Burgy, and V. Malka, Nature (London) **431**, 541 (2004).

[4] E. Miura, K. Koyama, S. Kato, N. Saito, M. Adachi, Y. Kawada, T. Nakamura, and M. Tanimoto, Appl. Phys. Lett. **86**, 251501 (2005).

[5] W. P. Leemans, B. Nagler, A. J. Gonsalves, C. Toth, K. Nakamura, C. G. R. Geddes, E. Esarey, C. B. Schroeder, and S. M. Hooker, Nature Phys. **2**, 696 (2006).

[6] S. Karsch, J. Osterhoff, A. Popp, T. P. Rowlands-Rees, Zs. Major, M. Fuchs, B. Marx, R. Horlein, K. Schmid, L. Veisz, S. Becker, U. Schramm, B. Hidding, G. Pretzler, D. Habs, F. Gruner, F. Krausz, and S. M. Hooker, New J. Phys. **9**, 415 (2007).

[7] X. Wang, R. Zgadzaj, N. Fazel, Z. Li, S. A. Yi, Xi Zhang, W. Henderson, Y.-Y. Chang, R. Korzekwa, H.-E. Tsai, C.-H. Pai, H. Quevedo, G. Dyer, E. Gaul, M. Martinez, A. C. Bernstein, T. Borger, M. Spinks, M. Donovan, V. Khudik, G. Shvets, T. Ditmire, and M. C. Downer, Nature Commun. **4**, 1988 (2013).

[8] W. P. Leemans, A. J. Gonsalves, H.-S. Mao, K. Nakamura, C. Benedetti, C. B. Schroeder, Cs. Toth, J. Daniels, D. E. Mittelberger, S. S. Bulanov, J.-L. Vay, C. G. R. Geddes, and E. Esarey, Phys. Rev. Lett. **113**, 245002 (2014).

[9] K. Krushelnick, Z. Najmudin, S. P. D. Mangles, A. G. R. Thomas, M. S. Wei, B. Walton, A. Gopal, E. L. Clark, A. E. Dangor, S. Fritzler, C. D. Murphy, P. A. Norreys, W. B. Wei, J. Gallacher, D. Jaroszynski, and R. Viskup, Phys. Plasmas **12**, 056711 (2005).

[10] W. L. Kruer, *The Physics of Laser Plasma Interaction* (Addison Wesley, Boston, 1998).

[11] C. S. Liu and V. K. Tripathi, *The Interaction of Electromagnetic Waves with Electron Beams and Plasmas* (World Scientific, Singapore, 1994)

[12] P. Gibbon, *Short Pulse Laser Interaction with Matter* (World Scientific, Singapore, 2005).

[13] T. Hosokai, K. Kinoshita, A. Zhidkov, A. Maekawa, A. Yamazaki, and M. Uesaka, Phys. Rev. Lett. **97**, 075004 (2006).

[14] T. Hosokai, A. Zhidkov, A. Yamazaki, Y. Mizuta, M. Uesaka, and R. Kodama, Appl. Phys. Lett. **96**, 121501 (2010).

[15] N. Nakanii, T. Hosokai, K. Iwasa, S. Masuda, A. Zhidkov, N. Pathak, H. Nakahara, Y. Mizuta, N. Takeguchi, and R. Kodama, Phys. Rev. ST Accel. Beams **18**, 021303 (2015).

[16] Y. Mizuta, T. Hosokai, S. Masuda, A. Zhidkov, K. Makito, N. Nakanii, S. Kajino, A. Nishida, M. Kando, M. Mori, H. Kotaki, Y. Hayashi, S. V. Bulanov, and R. Kodama, Phys. Rev. ST Accel. Beams **15**, 121301 (2012).

[17] S. Takeuchi, R. Sugihara, and K. Shimoda, J. Phys. Soc. Jpn. **63**, 1186 (1994).

[18] E. Esarey, P. Sprangle, and J. Krall, Phys. Rev. E **52**, 5443 (1995).

[19] Q. Kong, S. Miyazaki, S. Kawata, K. Miyauchi, K. Nakajima, S. Masuda, N. Miyanaga, and Y. K. Ho, Phys. Plasmas **10**, 4605 (2003).

[20] J. Vieira and J. T. Mendonca, Phys. Rev. Lett. **112**, 215001 (2014).

[21] N. Pathak, A. Zhidkov, N. Nakanii, S. Masuda, T. Hosokai, and R. Kodama, Phys. Plasmas **23**, 033102 (2016).

[22] D. Kaganovich, A. Ting, D. F. Gordon, R. F. Hubbard, T. G. Jones, A. Zigler, and P. Sprangle, Phys. Plasmas **12**, 100702 (2005).

[23] W. D. Kimura, A. van Steenbergen, M. Babzien, I. Ben-Zvi, L. P. Campbell, D. B. Cline, C. E. Dilley, J. C. Gallardo, S. C. Gottschalk, P. He, K. P. Kusche, Y. Liu, R. H. Pantell, I. V. Pogorelsky, D. C. Quimby, J. Skaritka, L. C. Steinhauer, and V. Yakimenko, Phys. Rev. Lett. **86**, 4041 (2001).

[24] T. Tajima, Proc. Jpn. Acad. Ser. B Phys. Biol. Sci. **86**, 147 (2010).

[25] H. Tomizawa and M. Kobayashi, *Proceedings of 29th International FEL Conference, WEPPH022* (Budker INP, Novosibirsk, 2007), p. 382.

[26] A. Maekawa, M. Uesaka, and H. Tomizawa, *Proceedings of 30th International FEL Conference, TUPPH082* (Pohang Accelerator Laboratory, Gyeongju, 2008), p. 435.

[27] S. V. Bulanov, I. N. Inovenkov, V. I. Kirsanov, N. M. Naumova, and A. S. Sakharov, Phys. Fluids B **4**, 1935 (1992).

[28] A. Giulietti *et al.*, Phys. Plasmas **20**, 082307 (2013).

[29] V. Malka, A. Modena, Z. Najmudin, A. E. Dangor, C. E. Clayton, K. A. Marsh, C. Joshi, C. Danson, D. Neely, and F. N. Walsh, Phys. Plasmas **4**, 1127 (1997).

[30] A. G. Zhidkov, T. Fujii, and K. Nemoto, Phys. Rev. E **78**, 036406 (2008).

[31] J. A. Stamper, R. H. Lehmberg, A. Schmitt, M. J. Herbst, F. C. Young, J. H. Gardner, and S. P. Obenschain, Phys. Fluids **28**, 2563 (1985).